Preparation, characterization, and biological activity study of thymoquinone-cucurbit[7]uril inclusion complex

Lubna Alrawashdeh,*[a] Khaleel I. Assaf, [iD] *[b] Walhan Alshaer, [iD] [c] Fadwa Odeh[d] and Suhair A. Bani-Atta[e]

In this study, the formation of a host–guest inclusion complex between cucurbit[7]uril (CB[7]) and thymoquinone (TQ) was investigated in aqueous solution. The formation of a stable inclusion complex, CB[7]–TQ, was confirmed by using different techniques, such as ^{1}H NMR and UV-visible spectroscopy. The aqueous solubility of TQ was clearly enhanced upon the addition of CB[7], which provided an initial indication for supramolecular complexation. The complexation stoichiometry and the binding constant of the inclusion complex were determined through a combination of two sets of titration methods, including UV-visible and fluorescence displacement titrations. Both methods suggested the formation of a 1 : 1 stoichiometry between CB[7] and TQ with moderate binding affinity of 3×10^3 M^{-1}. Density functional theory (DFT) calculations were also performed to verify the structure of the resulted host–guest complex and to support the complexation stoichiometry. The theoretical calculations were in agreement with experimental results obtained by ^{1}H NMR spectroscopy. Most importantly, the cytotoxic effect of the CB[7]–TQ complex was investigated against cancer and normal cell lines. The results showed that the anticancer activity of TQ against MDA-MB-231 cells was enhanced by the complexation with CB[7], while no significant effect was observed in MCF-7 cells. The results also confirmed the low toxicity of the CB[7] host molecule that supports the use of CB[7] as a drug carrier.

Introduction

Nigella sativa (also called black seed or black cumin) is a promising medicinal plant, especially in the Mediterranean region and Western Asian countries including India, Pakistan, and Afghanistan.[1,2] It has been used to treat a range of health conditions for many years, such as lung diseases, arthritis, and hypercholesterolemia. The biological activity of *nigella sativa* is mainly related to one of its main active components, namely, thymoquinone (TQ, 2-isopropyl-5-methylbenzo-1,4-quinone, Fig. 1).[3] Several studies have been established to investigate the therapeutic effect of TQ. These studies showed strong indications that TQ has a very interesting and significant therapeutic effect in cancer, inflammation, and as an antioxidant

agent through different modes of action. For example, TQ is able to arrest tumor cells at different stages of their progression.[2] Recently, TQ showed a potential inhibition activity against coronavirus infections.[4,5]

Despite the promising therapeutic efficiency of TQ, the lack of bioavailability, pharmacokinetic parameters, and formulation problems deferred the usage of TQ in the clinical development.[3] The bioavailability problem (for example, poor solubility in water) is mainly related to the fact that TQ is a hydrophobic molecule. In addition, it has been reported that TQ has stability problems in solution; in particular, TQ is very sensitive to heat and light.[6] Many attempts have been done to
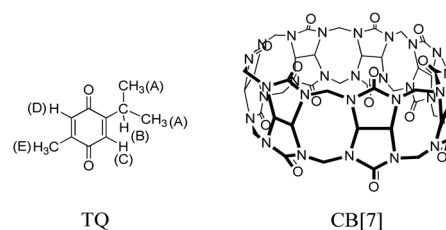
[a]*Department of Chemistry, Faculty of Science, The Hashemite University, P.O. Box 330127, Zarqa, 13133, Jordan. E-mail: lubna.reyad@hu.edu.jo*

[b]*Department of Chemistry, Al-Balqa Applied University, Al-Salt, 19117, Jordan. E-mail: khaleel.assaf@bau.edu.jo*

[c]*Cell Therapy Center, The University of Jordan, Amman, 11942, Jordan*

[d]*Department of Chemistry, School of Science, The University of Jordan, Amman, 11942, Jordan*

[e]*Department of Chemistry, Faculty of Science, University of Tabuk, 71491, Saudi Arabia*

Fig. 1 Structure of thymoquinone (TQ, left), and cucurbit[7]uril (CB[7], right).

overcome the bioavailability and stability difficulties. The most important attempt was established by encapsulating TQ within different nanomaterials (vehicles/carriers). For example, several drug delivery systems were used, such as liposomes,[7] lipids,[8] cyclodextrins (CDs),[9,10] nanoparticles,[11] *etc.* These studies showed that encapsulation of TQ within the new environments (carrier/vehicle) can improve its bioavailability, stability (thermal/light), and activity as an anti-cancer agent.

In this work, we are interested in introducing another and new host molecule to TQ, for the purpose of defining possible improvements in the performance of TQ pharmaceutical properties when associated with this host. Then we compare the obtained results with the previous studies that used different host molecules. Cucurbit[*n*]urils (CB[*n*], Fig. 1) are another attractive class of water soluble macrocyclic host molecules, which, like CDs and calixarenes, have a cavity that can accommodate different sizes of hydrophobic guest molecules.[12] CBs are composed of a different number of glycoluril units (*n* = 5–10) joined by pairs of methylene bridges.[13,14] The members of this family have a pumpkin shaped, highly symmetrical and rigid structure. They also possess a hydrophobic cavity and two identical partially-negatively charged carbonyl portals (hydrophilic).[15] The binding of guest molecules to CB[*n*] can be driven by ion-dipole, and dipole–dipole interactions (suitable for cationic moiety parts), or through the hydrophobic effect (suitable to bind neutral and hydrophobic residues).[16] Cucurbit [7]uril (CB[7], Fig. 1) is the most soluble member of the CB[*n*] family.[14,17]

Recent studies start to give notable interest to the CB[*n*] family in the biological and medicinal fields.[18] Particular focus has been given to the CB[*n*] family in the drug delivery area, and many studies have been using CB[*n*]-type molecular hosts as a drug delivery vehicle for a large number of drugs.[19] Based on the previous studies, it has been suggested that CB[*n*] showed significant advantages over the CD host molecule, which is the most common choice in the drug delivery area. For example, the binding constants (*K*) of CB[*n*]-guest complexes are higher than those of CDs in aqueous medium.[20] Also, the encapsulation of drug molecules in CB[*n*] provides a method for slow drug release, facilitate drug targeting, improve chemical and thermal stability, reduction in toxicity, and enhance the aqueous solubility of poorly soluble drugs. Most importantly, CBs are a promising drug delivery system, being non-toxic and highly biocompatible.[20,21]

Herein, we report for the first time the formation of a stable inclusion complex between TQ and CB[7] in aqueous solution. The complexation is investigated by ^{1}H NMR and UV-visible spectroscopy. The binding constant is determined by using UV-visible and fluorescence displacement titrations. In addition, a theoretical evaluation of the CB[7]–TQ inclusion complex stoichiometry and energy measurements are performed. Moreover, the antiproliferative effect of the CB[7], TQ, and CB[7]–TQ complex is investigated against two breast cancer cell lines, MDA-MB-231 and MCF-7, and compared to the effect against human dermal fibroblast cell line, HDF, to evaluate retaining toxicity of TQ after complexation with CB[7]. A previously

reported βCD–TQ complex was used for comparison with CB[7]–TQ.

Experimental section

Chemicals and instruments

Thymoquinone, acridine orange base (AO), β-cyclodextrin (βCD) and D_2O (99 atom % D) were purchased from Sigma-Aldrich (USA). Cucurbit[7]uril (CB[7]) was prepared according to literature.[22] All reagents and chemicals were used without further treatment. ^{1}H NMR spectra were performed on a Bruker AVANCE-III 400 MHz NanoBay FT-NMR spectrometer, in D_2O and referenced in ppm with respect to a tetramethylsilane (TMS). The UV-visible absorption spectra were measured on Cary-100 Bio instrument. Fluorescence experiments were performed using Jasco spectrofluorometer (FP-6500).

^{1}H NMR titration of TQ and CB[7]

CB[7] stock solution (host) was prepared by dissolving 0.01 g of CB[7] in 0.7 mL D_2O, heating and sonication were used to speed the dissolution; the CB[7] concentration was corrected to 80% content. The CB[7] solution was then filtrated using syringe filter (0.45 μm, nylon). Different aliquots of CB[7] stock solution were then added into a solution of TQ (9.7 mM) in D_2O to obtain 1 : 1 ratio of CB[7] : TQ.

UV-visible titration of TQ and CB[7]: complexation stoichiometry and binding study

Stock solution of CB[7] was prepared first (11 mM), different aliquots of CB[7] stock solution were added to a solution of TQ (1 mM). The UV-visible spectrum was recorded after each addition until getting a 1 : 1 ratio of CB[7] : TQ. The complexation stoichiometry and the binding constant of CB[7]–TQ inclusion complex were determined using the Benesi–Hildebrand equation based on the data from UV-visible spectrophotometry. Eqn (1) and (2) were used for 1 : 1 and 1 : 2 binding models.

$$\frac{1}{A - A^\circ} = \frac{1}{A' - A^\circ} + \frac{1}{K(A' - A^\circ)[\text{host}]} \quad (1)$$

$$\frac{1}{A - A^\circ} = \frac{1}{A' - A^\circ} + \frac{1}{K(A' - A^\circ)[\text{host}]^2} \quad (2)$$

According to the design of Benesi–Hildebrand experiment, A° is absorbance of the free TQ, while A is absorbance at different CB[7] concentrations, A' is absorbance at the maximum concentration of the host. The association constant (K) is calculated from the Benesi–Hildebrand equation, after plotting $(1/A - A^\circ)$ against $(1/[\text{host}])$ for 1 : 1 (host : guest stoichiometric ratio), or $(1/[\text{host}]^2)$ for 1 : 2 (host : guest stoichiometric ratio). Binding constant is then calculated as:

$$K = \frac{1}{\text{Slope}(A' - Y^\circ)} \quad (3)$$

Fluorescence titration of CB[7] with AO dye and binding constant of CB[7]–AO inclusion complex

An aqueous solution contains CB[7] and AO (1 mM CB[7] and 1 μM AO dye) was prepared first. Different aliquots of this solution were added into a solution of AO (1 μM). The emission peak of AO at $\lambda_{em} = 521$ nm ($\lambda_{ex} = 470$ nm) was followed to study the effect of adding CB[7] on the emission of AO. The additions were stopped after obtaining a plateau in the experimental fluorescence data. Binding constant of CB[7]–AO inclusion complex was obtained by fitting the titration data[20,21] at $\lambda_{em} = 510$ nm by using Origin program.

Displacement titration and binding constant of CB[7]–TQ inclusion complex

An aqueous solution contains 10 μM CB[7] and 1 μM AO dye, was prepared first. Then, a solution of 10 μM CB[7], 1 μM AO dye, and 1.6 mM TQ was prepared. For displacement titration, different aliquots of TQ solution were added into the first solution (CB[7]–AO). The emission peak of AO encapsulated species at $\lambda_{em} = 510$ nm ($\lambda_{ex} = 470$ nm) was followed to study the effect of adding TQ on the emission. The additions were stopped after obtaining a plateau in the experimental fluorescence data. Binding constant of CB[7]–TQ inclusion complex was obtained by fitting the titration data[22,23] at $\lambda_{em} = 510$ nm by using Origin program.

Quantum chemical calculations

Density functional theory (DFT) calculations were performed using Gaussian 09.[23] The dispersion-correct DFT method (wB97XD)[24] was used with the 6-31G* basis set. All calculations were performed in the gas phase.

Cells culture

Human breast adenocarcinoma (MDA-MB-231) and human dermal fibroblast (HDF) cell lines were cultured in Dulbecco's Modified Eagle Medium (DMEM) (Euroclone SpA, Italy), while Human breast cancer (MCF-7) cell line was cultured in RPMI-1640 medium (Euroclone SpA, Italy). Both DMEM and RPMI-1640 were supplemented with 10% (v/v) fetal bovine serum (FBS), 100 U mL^{-1} penicillin, 100 mg mL^{-1} streptomycin, and 2 mM L-glutamine, and maintained in an incubator (Memmert, Germany) at 37 °C under an atmosphere of 5% CO$_2$ and 90% relative humidity. The cells were sub-cultivated approximately every 2 to 3 days using 0.05% (w/v) trypsin-EDTA.

Cell viability assay

MDA-MB-231, MCF-7 and HDF (5 × 10^3 cells per well) were seeded in 96-well plates. After 24 h, the cells were treated with serial dilution of each of the CB[7], βCD, TQ, βCD–TQ complex, CB[7]–TQ complex in a concentration range of 0 to 1000 μM for 72 h (the host–guest solutions were prepared in 1 : 1 molar ratio). After 72 h of incubation at 37 °C, treatment was removed from the wells, followed by adding 15 μL of 3-(4,5-dimethyl-2-thiazolyl)-2,5-diphenyltetrazolium Bromide (MTT) solution and 100 μL of the medium. After 3 h of incubation, the medium

was removed, then 50 μL of dimethyl sulfoxide (DMSO) was added for dissolving the formazan. The absorbance was measured at a wavelength of 570 nm using Glomax microplate reader (Promega, USA).

Results and discussion

CB[7]–TQ inclusion complex

The inclusion complex between TQ and CB[7] (structures shown in Fig. 1) was investigated using several spectroscopic methods. In particular, NMR is a very powerful technique for studying guest–host complexation since it is highly influenced by any changes in the microenvironment of the nucleus under study in addition to its chemical identity capabilities. Several NMR experiments are useful in gaining insights on type and location of interaction between molecules such as the chemical shift ($\Delta\delta$), relaxation time (T_1) and diffusion measurements (DOSY experiments). However, simple ^{1}H NMR experiments to observe chemical shift changes upon complexation (or interaction) are very efficient. The ^{1}H NMR spectrum of free TQ in D$_2$O is shown in Fig. 2a, the protons' signals are broadened due to the low solubility of TQ in water, and the possible aggregation.

Upon the addition of different aliquots of CB[7] to TQ solution, the proton of the guest experienced complexation induced chemical shifts ($\Delta\delta$), and the shape of the signals changed suggesting the formation of CB[7]–TQ inclusion complex. As shown in Table 1, a significant upfield shift was noticed in H_A, H_B and H_C signals of TQ ($+\Delta\delta = 0.66, 0.89, 0.84$ ppm, respectively), this indicated that these protons are accommodated deep inside the CB[7] cavity, and that the observed upfield shift is related to the shielding effect of the hydrophobic cavity of CB[7].[16,25] On the other hand, protons H_D and H_E are positioned out of the cavity of CB[7], and close to the carbonyl rims, as indicated by the downfield shift ($-\Delta\delta$).[25] In addition, the shape of TQ protons in the ^{1}H NMR spectra was largely affected by CB[7] additions. The signals (protons B, C, D and E) in D$_2$O were broad (Fig. 2a), indicating their presence in an aggregated state
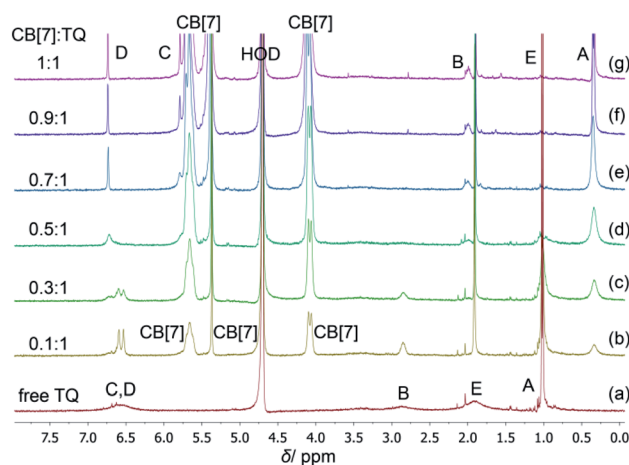

Fig. 2 ^{1}H NMR titration of TQ and CB[7], (a) the spectrum of free TQ, (b–g) the spectra of CB[7]–TQ at different molar ratio, in D$_2$O at ambient temperature.

Table 1 Chemical shift difference ($\Delta\delta$) in ppm of ^{1}H NMR resonances of free TQ compared to the 1 : 1 CB[7]–TQ inclusion complex in D_2O at ambient temperature

| Proton	δ_{TQ}	$\delta_{(TQ\,:\,CB[7])}$	$\Delta\delta^a$
A	1.00	0.34	0.66
B	2.88	1.99	0.89
C	6.62	5.78	0.84
D	6.62	6.73	−0.11
E	1.88	1.90	−0.02

^{a} A positive $\Delta\delta$ indicates an upfield shift.

and not as free hydrated TQ molecules. This behavior has been reported in literature regarding self-assembly of small organic molecules in aqueous solutions.[26] Upon the addition of CB[7], an enhancement in solubility is achieved due to complexation and the aggregates start breaking giving sharp ^{1}H NMR signals (Fig. 2b–g).[27] No further shift in the TQ peaks was noticed after reaching 1 : 1 mole ratio (host:guest), which indicated the formation of 1 : 1 stable inclusion complex of CB[7]–TQ. The gradual disappearance of some signals of free TQ and the appearance of CB[7]–TQ inclusion complex signals, suggested slow exchange on the NMR time scale.

The formation of inclusion complex CB[7]–TQ was further investigated by using UV-visible spectroscopy. The free TQ showed two absorption peaks, at 334 nm and at 434 nm (as a shoulder) in aqueous medium. As shown in Fig. 3a, addition of CB[7] into the TQ solution (1 mM) resulted in gradually decrease of the absorption peak at ∼334 nm (λ_{max} of the free TQ) until almost disappeared at 1 : 1 mole ratio of CB[7] : TQ. Also, a decrease in the absorbance of the shoulder peak of TQ (λ = 434 nm) with bathochromic shift (from 434 nm to 447 nm) was observed upon CB[7] addition. These changes confirmed the formation of host–guest inclusion complex (CB[7]–TQ complex).[25]

Complexation stoichiometry and binding constant determination
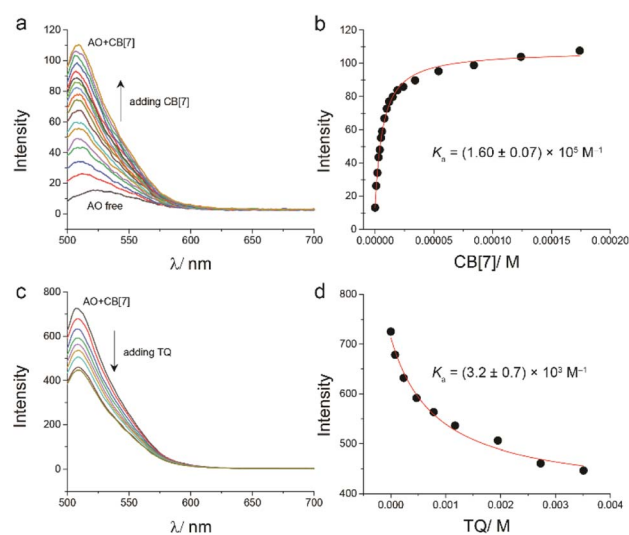
The UV-visible spectrophotometry was used to investigate the host–guest complex formation of CB[7]–TQ, the spectra obtained for successive additions of CB[7] to TQ in aqueous solution are shown in Fig. 3a. The complexation stoichiometry
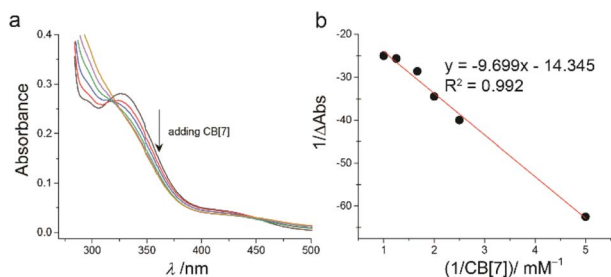
and the binding constant of CB[7]–TQ inclusion complex were determined using the Benesi–Hildebrand equation based on the titration data from UV-visible spectrophotometry.[28] A linear dependence of the type $1/(A - A^\circ)$ *vs.* $1/[CB7]^n$, with $n = 1$, indicated the presence of 1 : 1 stoichiometry of the CB[7] : TQ complex. Fig. 3b represents the Benesi–Hildebrand plot for CB[7]–TQ inclusion complex using UV-visible spectrophotometric titration for 1 : 1 stoichiometry. A Good linear correlation was obtained for $n = 1$ (Fig. 3b), with a binding constant (K) of 2.5×10^3 M^{-1}. Fitting the data according to nonlinear model also provided a K of 3×10^3 M^{-1}.

The binding of TQ and CB[7] was also investigated using optical dye displacement titration. This method relies on the competitive displacement of a fluorescent dye from a host molecule by the guest we intend to study.[29,30] Different dyes were used in the indicator displacement titration with CB[7].[31,32] In this study, acridine orange dye (AO) was used for this purpose. Upon the addition of CB[7] to aqueous solution of AO, a blue shift (from $\lambda_{em} = 521$ nm for free AO, to $\lambda_{em} = 510$ nm after adding CB[7]) and a large enhancement in the emission peak of AO were observed (Fig. 4a). The binding constant of CB[7]–AO inclusion was found to be 1.6×10^5 M^{-1} based on the titration experiment (Fig. 4b), which is in line with the reported value.[15]

For displacement titration, different aliquots of TQ solution were added into an aqueous solution of the encapsulated adduct CB[7]–AO, a continuous decrease in the emission spectrum of CB[7]–AO was observed (Fig. 4c). The addition of TQ was stopped after reaching a plateau in the experiment data, which confirmed reaching the equilibrium between the encapsulated and the free TQ. By fitting the data of fluorescence displacement titration experiment (adding TQ to CB[7]–AO solution), the value of the binding constant of CB[7] and TQ was obtained ($K = 3.2 \times 10^3$ M^{-1}) (Fig. 4d). This value was almost similar to the value obtained from UV-visible titration (2.5×10^3 M^{-1}).

Fig. 3 The UV-visible absorbance spectra of the titration experiment of TQ (1 mM) and CB[7] in water at ambient temperature (a), Benesi–Hildebrand plots of 1/ΔAbs *versus* 1/[CB7] for CB[7]–TQ inclusion complex using UV-visible titration data (b).

Fig. 4 (a) Fluorescence titration spectra of AO (1 μM) with different concentrations of CB[7], (b) fitted titration data of AO with CB[7], (c) the displacement titration of TQ and CB[7]–AO, (d) fitted titration data of the displacement titration of TQ with CB[7]–AO.

DFT calculations

The optimized structures of the free TQ, CB[7], and the CB[7]–TQ complex are shown in Fig. 5. The cavity volume of CB[7] (242 $Å^3$) can accommodate only one residue of TQ (size 161 $Å^3$), resulting in a packing coefficient (PC% = guest size/cavity volume) of 67%, which verified the experimentally observed 1 : 1 binding stoichiometry. The calculations showed the formation of an inclusion complex was stabilized by -37 kcal mol^{-1} in the gas phase compared to the free components. The obtained structure of the CB[7]–TQ complex showed that the benzoquinone was fully encapsulated inside the hydrophobic cavity of CB[7], while the methyl substituent was positioned inside the cavity and close to the carbonyl rim. In contrast, the isopropyl substituent was partial excluded and more exposed to the surrounding. These structural results are in line with the ^{1}H NMR data.

Cytotoxicity

The cytotoxic effect of the CB[7]–TQ complex was investigated against breast cancer using MTT assay. Moreover, the toxicity of the CB[7], βCD, free TQ, and βCD–TQ complex were assessed and compared to CB[7]–TQ complex. To do so, triple-negative human breast cancer cell line (MDA-MB-231), estrogen receptor (ER)-positive human breast cancer cell line (MCF-7), and normal human dermal fibroblast cell line (HDF) were used. The three cell lines were treated with different concentrations of CB[7], βCD, free TQ, βCD–TQ complex, or CB[7]–TQ complex for 72 h. In general, the results revealed higher toxicity for free TQ, βCD–TQ complex, and CB[7]–TQ complex to both breast cancer cell lines (Fig. 6a, b) compared to normal fibroblast (Fig. 6c). Furthermore, based on IC$_{50}$ values (Table 2), it was noticed that the toxicity of βCD–TQ and CB[7]–TQ complexes was higher than the free TQ in MDA-MB-231 cells compared to no significant differences in the cytotoxicity of TQ, βCD–TQ complex, and CB[7]–TQ complexes in MCF-7 cells (Table 2). Importantly, there was no significant toxicity against the three tested cell lines obtained from βCD and CB[7] treatment. All of these results confirmed that the anticancer activity of TQ was almost not affected by the kind of the host molecule that used to form the inclusion complexes (based on IC$_{50}$ values, Table 2). An interesting finding in the current work was the similar antiproliferative effect of TQ when complexed with CB[7] or βCD counterparts. The similar effect is most likely due to the formation of 1 : 1 inclusion complexes and the ability of both CB[7] and βCD to deliver and release of TQ into the cells in a similar manner. Moreover, an intensive and comparative
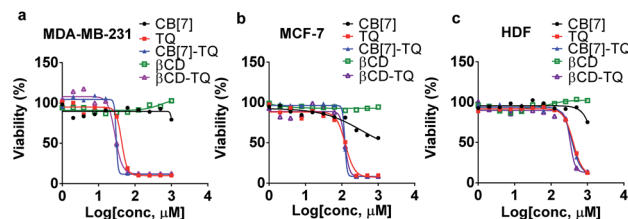

Fig. 6 The dose−response curves of CB[7], βCD, TQ, βCD–TQ complex, CB[7]–TQ complex. (a) MDA-MB-231, (b) MCF-7 and (c) HDF cells were treated with serial concentrations of CB[7], βCD, TQ, βCD–TQ complex, CB[7]–TQ complex for 72 h. The cell viability was determined by the MTT assay. Data mean ± SD ($n = 3$).

study of uptake and release of TQ from CB[7] and βCD is of high interest for more understanding.

The antiproliferative activity of TQ loaded into different nanocarriers have been described by several studies and have been shown either higher or equal activity in comparison to free TQ.[9,33–37] For instance, Bhattacharya *et al.* reported similar antiproliferative effect of TQ-loaded into polymeric nanoparticles against MCF7 when compared to free TQ.[37] Moreover, Ganea *et al.* reveled twofold higher toxicity of TQ-loaded into PLGA nanoparticles in MDA-MB-231 cells compared to free TQ.[35] In contrary, Odeh *et al.* showed that the encapsulation of TQ in βCD, enhanced its antiproliferative activity against MCF7.[9] Encapsulation of TQ in liposomes also enhanced its solubility and hence its bioavailability against MCF7 and MDA-MB-231 cell lines.[7]

The TQ's mode of action on different cell lines is an important factor in deciding the suitable carrier aside from enhanced solubility and bioavailability. For example, Sunoqrot *et al.* reported the encapsulation of TQ in polymeric particles and tested their activity on various cell lines.[38] Their results showed no enhancement of the antiproliferative activity of TQ-polymer compared to free TQ, but the selectivity index and *in vivo* bioavailability were more prominent. TQ, either free, encapsulated in a nanocarrier or in combination with other chemotherapeutics, is very promising against many cancers including cancer stem cells.[39–41] Moreover, the results also confirmed the low toxicity of CB[7] that supports the use of CB[7] as a drug carrier. Previously described reports about toxicity and safety of CB[n] demonstrated the relative safety and acceptable toxicity *in vitro* and *in vivo*.[42,43] For example, Oun *et al.* reported the lack of significant tissue specific toxicity of CB[6] and CB[7] using ex
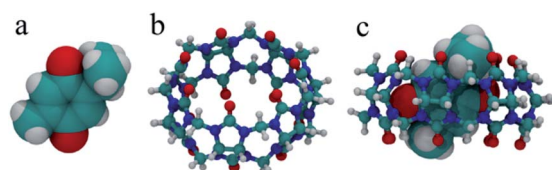

Fig. 5 DFT-optimized structures of (a) TQ, (b) CB[7], and (c) CB[7]−TQ complex in gas phase.

Table 2 Summary of IC$_{50}$ values for CB[7], βCD, TQ, βCD–TQ complex, CB[7]–TQ complex, see Fig. 6

	IC$_{50}$ ± SD (μM, $n = 3$)		
	MDA-MB-231	MCF-7	HDF
CB[7]	>1000	>1000	>1000
βCD	>1000	>1000	>1000
TQ	42.5 ± 1.5	123.7 ± 11.3	407.9 ± 14.0
CB[7]–TQ	29.2 ± 1.7	118.3 ± 8.8	370.8 ± 33.3
βCD–TQ	28.6 ± 2.7	121.3 ± 6.2	332.3 ± 19.9

vivo rat model.[42] Moreover, Hettiarachchi *et al.* revealed the very low toxicity of CB[5] and CB[7] and high cell tolerance at concentrations of up to 1 mM when tested against normal human cell lines originated from kidney, liver, and blood tissues.[43]

Conclusion

The inclusion complex CB[7]–TQ was successfully prepared in 1 : 1 mole ratio of CB[7] : TQ with moderate strength binding (K of 3×10^3 M^{-1}) in aqueous solution. As a result of this inclusion process, the solubility of TQ was clearly enhanced (based on ^{1}H NMR spectroscopy study), which is useful in increasing the bioavailability of TQ in aqueous solution. The experimental and computational theoretical results are consistent with inclusion of a single TQ molecule within CB[7] cavity. The cytotoxic effect of the CB[7]–TQ complex was investigated against cancer and normal cell lines, which revealed that the anticancer activity of TQ can be enhanced by forming a stable inclusion complex with CB[7]. Results showed also that the anticancer activity of TQ was not affected by the kind of the host molecule that used in the complexation process. Overall, the results highlight the potential implementation of supramolecular complexation in medicinal chemistry and drug delivery applications.

Conflicts of interest

There are no conflicts to declare.

Acknowledgements

References

1 C. C. Woo, A. P. Kumar, G. Sethi and K. H. B. Tan, *Biochem. Pharmacol.*, 2012, **83**, 443–451.

2 S. Banerjee, S. Padhye, A. Azmi, Z. Wang, P. A. Philip, O. Kucuk, F. H. Sarkar and R. M. Mohammad, *Nutr. Cancer*, 2010, **62**, 938–946.

3 S. Darakhshan, A. Bidmeshki Pour, A. Hosseinzadeh Colagar and S. Sisakhtnezhad, *Pharmacol. Res.*, 2015, **95–96**, 138–158.

4 H. Xu, B. Liu, Z. Xiao, M. Zhou, L. Ge, F. Jia, Y. Liu, H. Jin, X. Zhu, J. Gao, J. Akhtar, B. Xiang, K. Tan and G. Wang, *Infect. Dis. Ther.*, 2021, **10**, 483–494.

5 S. Elgohary, A. A. Elkhodiry, N. S. Amin, U. Stein and H. M. El Tayebi, *Cells*, 2021, **10**, 302.

6 J. M. M. Salmani, S. Asghar, H. Lv and J. Zhou, *Molecules*, 2014, **19**, 5925–5939.

7 F. Odeh, S. I. Ismail, R. Abu-Dahab, I. S. Mahmoud and A. Al Bawab, *Drug Delivery*, 2012, **19**, 371–377.

8 S. I. Abdelwahab, B. Y. Sheikh, M. M. E. Taha, C. W. How, R. Abdullah, U. Yagoub, R. El-Sunousi and E. E. M. Eid, *Int. J. Nanomed.*, 2013, **8**, 2163–2172.

9 R. Abu-Dahab, F. Odeh, S. I. Ismail, H. Azzam and A. Al Bawab, *Pharmazie*, 2013, **68**, 939–944.

10 M. S. Al-Qubaisi, A. Rasedee, M. H. Flaifel, E. E. M. Eid, S. Hussein-Al-Ali, F. H. Alhassan, A. M. Salih, M. Z. Hussein, Z. Zainal, D. Sani, A. H. Aljumaily and M. I. Saeed, *Eur. J. Pharm. Sci.*, 2019, **133**, 167–182.

11 V. K. Kumar, R. R. Devi and E. Hemananthan, *J. Dispersion Sci. Technol.*, 2020, **41**, 243–256.

12 H. Yin, D. Bardelang and R. Wang, *Trends Chem.*, 2021, **3**, 1–4.

13 A. L. Koner and W. M. Nau, *Supramol. Chem.*, 2007, **19**, 55–66.

14 K. I. Assaf and W. M. Nau, *Chem. Soc. Rev.*, 2015, **44**, 394–418.

15 M. Shaikh, J. Mohanty, P. K. Singh, W. M. Nau and H. Pal, *Photochem. Photobiol. Sci.*, 2008, **7**, 408–414.

16 K. I. Assaf, M. Florea, J. Antony, N. M. Henriksen, J. Yin, A. Hansen, Z. W. Qu, R. Sure, D. Klapstein, M. K. Gilson, S. Grimme and W. M. Nau, *J. Phys. Chem. B*, 2017, **121**, 11144–11162.

17 E. Masson, X. Ling, R. Joseph, L. Kyeremeh-Mensah and X. Lu, *RSC Adv.*, 2012, **2**, 1213–1247.

18 H. S. El-Sheshtawy, S. Chatterjee, K. I. Assaf, M. N. Shinde, W. M. Nau and J. Mohanty, *Sci. Rep.*, 2018, **8**, 1–10.

19 K. I. Kuok, S. Li, I. W. Wyman and R. Wang, *Ann. N. Y. Acad. Sci.*, 2017, **1398**, 108–119.

20 D. Das, K. I. Assaf and W. M. Nau, *Front. Chem.*, 2019, **7**, 619.

21 A. I. Day and A. S. Atthar, in *Cucurbiturils and Related Macrocycles*, The Royal Society of Chemistry, 2020, pp. 238–282.

22 A. Day, A. P. Arnold, R. J. Blanch and B. Snushall, *J. Org. Chem.*, 2001, **66**, 8094–8100.

23 M. J. Frisch, G. W. Trucks, H. B. Schlegel, G. E. Scuseria, M. A. Robb, J. R. Cheeseman, G. Scalmani, V. Barone, B. Mennucci, G. A. Petersson, H. Nakatsuji, M. Caricato, X. Li, H. P. Hratchian, A. F. Izmaylov, J. Bloino, G. Zheng, J. L. Sonnenberg, M. Hada, M. Ehara, K. Toyota, R. Fukuda, J. Hasegawa, M. Ishida, T. Nakajima, Y. Honda, O. Kitao, H. Nakai, T. Vreven, J. A. Montgomery Jr, J. E. Peralta, F. Ogliaro, M. Bearpark, J. J. Heyd, E. Brothers, K. N. Kudin, V. N. Staroverov, T. Keith, R. Kobayashi, J. Normand, K. Raghavachari, A. Rendell, J. C. Burant, S. S. Iyengar, J. Tomasi, M. Cossi, N. Rega, J. M. Millam, M. Klene, J. E. Knox, J. B. Cross, V. Bakken, C. Adamo, J. Jaramillo, R. Gomperts, R. E. Stratmann, O. Yazyev, A. J. Austin, R. Cammi, C. Pomelli, J. W. Ochterski, R. L. Martin, K. Morokuma, V. G. Zakrzewski, G. A. Voth, P. Salvador, J. J. Dannenberg, S. Dapprich, A. D. Daniels, O. Farkas, J. B. Foresman, and J. V. Ortiz, J. Cioslowski and D. J. Fox, *Gaussian 09*, Gaussian, Inc., Wallingford, CT, 2010.

24 T. C. Lee, E. Kalenius, A. I. Lazar, K. I. Assaf, N. Kuhnert, C. H. Grün, J. Jänis, O. A. Scherman and W. M. Nau, *Nat. Chem.*, 2013, **5**, 376–382.

25 G. H. Aryal, K. I. Assaf, K. W. Hunter, W. M. Nau and L. Huang, *Chem. Commun.*, 2017, **53**, 9242–9245.

26 F. Odeh, A. Al-Bawab and Y. Li, *J. Dispersion Sci. Technol.*, 2010, **31**, 162–168.

27 A. Thangavel, I. A. Elder, C. Sotiriou-Leventis, R. Dawes and N. Leventis, *J. Org. Chem.*, 2013, **78**, 8297–8304.

28 J. S. Negi and S. Singh, *Carbohydr. Polym.*, 2013, **92**, 1835–1843.

29 K. I. Assaf, O. Suckova, N. Al Danaf, V. Von Glasenapp, D. Gabel and W. M. Nau, *Org. Lett.*, 2016, **18**, 932–935.

30 A. Praetorius, D. M. Bailey, T. Schwarzlose and W. M. Nau, *Org. Lett.*, 2008, **10**, 4089–4092.

31 K. I. Assaf and W. M. Nau, *Supramol. Chem.*, 2014, **26**, 657–669.

32 S. Gupta, Y. Zhao, R. Varadharajan and V. Ramamurthy, *ACS Omega*, 2018, **3**, 5083–5091.

33 I. Fakhoury, W. Saad, K. Bouhadir, P. Nygren, R. Schneider-Stock and H. Gali-Muhtasib, *J. Nanopart. Res.*, 2016, **18**, 1–16.

34 H. Dehghani, M. Hashemi, M. Entezari and A. Mohsenifar, *Iran. J. Pharm. Res.*, 2015, **14**, 539–546.

35 G. M. Ganea, S. O. Fakayode, J. N. Losso, C. F. Van Nostrum, C. M. Sabliov and I. M. Warner, *Nanotechnology*, 2010, **21**, 285104.

36 J. Ravindran, H. B. Nair, B. Sung, S. Prasad, R. R. Tekmal and B. B. Aggarwal, *Biochem. Pharmacol.*, 2010, **79**, 1640–1647.

37 S. Bhattacharya, M. Ahir, P. Patra, S. Mukherjee, S. Ghosh, M. Mazumdar, S. Chattopadhyay, T. Das, D. Chattopadhyay and A. Adhikary, *Biomaterials*, 2015, **51**, 91–107.

38 S. Sunoqrot, M. Alfaraj, A. M. Hammad, V. Kasabri, D. Shalabi, A. A. Deeb, L. H. Ibrahim, K. Shnewer and I. Yousef, *Pharmaceutics*, 2020, **12**, 1–16.

39 F. R. Ballout and H. Gali-Muhtasib, *Pharmacogn. Rev.*, 2020, **14**, 155–159.

40 F. Odeh, R. Naffa, H. Azzam, I. S. Mahmoud, W. Alshaer, A. Al Bawab and S. Ismail, *Heliyon*, 2019, **5**, e02919.

41 M. M. Mehanna, R. Sarieddine, J. K. Alwattar, R. Chouaib and H. Gali-Muhtasib, *Int. J. Nanomed.*, 2020, **15**, 9557–9570.

42 R. Oun, R. S. Floriano, L. Isaacs, E. G. Rowan and N. J. Wheate, *Toxicol. Res.*, 2014, **3**, 447–455.

43 G. Hettiarachchi, D. Nguyen, J. Wu, D. Lucas, D. Ma, L. Isaacs and V. Briken, *PLoS One*, 2010, **5**, 2–11.

© 2022 The Author(s). Published by the Royal Society of Chemistry